ARTICLE

Electrodeposition of Nonconducting Polymers: Roles of Carbon Nanotubes in the Process and Products

Di Hu, Chuang Peng, and George Z. Chen*

Department of Chemical and Environmental Engineering, and Energy and Sustainability Research Division, Faculty of Engineering, University of Nottingham, Nottingham, NG7 2RD, U.K.

ABSTRACT The self-limiting electrodeposition of nonconducting polymers, such as poly(*o*-aminophenol) (P*o*AP), has been continued by the addition of acid treated carbon nanotubes (CNTs) into the aqueous monomer solution without any other supporting electrolyte. Electron microscopy revealed fairly thick (>8 μm) and highly porous nanocomposite films on electrodes, consisting of CNTs which were well interconnected and individually coated with a thin layer (*e.g.*, 30 nm) of the nonconducting polymer. The mechanism behind this approach is explainable by the newly arrived CNTs and those entrapped in the nonconducting polymer matrix providing extra reaction and growth sites, and extended electron pathways, leading to sustained electro-co-deposition of the nonconducting polymer and CNTs into the nanoporous composite films. Promising applications of the P*o*AP—CNT composite were explored, such as CO_2 sensing in water, and energy storage in an unprecedented metal-free supercapattery.

KEYWORDS: carbon nanotubes · nonconducting polymers · electrodeposition · CO_2 sensor · supercapattery

In contrast to conducting polymers, the electrosynthesis of nonconducting polymers is self-limited and inevitably ceases when the polymer film on the electrode grows thick enough to become too resistive for electron transfer between the electrode and the monomer molecules and radicals in the solution. As a consequence, the thickness of nonconducting polymer films was claimed to be only 10−100 nm,[1] depending on the real resistivity, which is much thinner than typical conducting polymer films (*e.g.*, 0.5 mm),[2] and continuous electrosynthesis is challenging. Although these thin nonconducting polymer films could be utilized in highly sensitive and selective sensors,[1,3−6] some reports indicated that the film thickness was too small to entrap an adequate amount of, for example, biomolecules.[7]

In the context of this work, the aforementioned "nonconducting" polymers are those with high resistivity and can be synthesized by electropolymerization in the presence of an electrolyte, such as acids, bases, or salts. Recently, anionic carbon nanotubes (CNTs) resulting from acid treatment have been successfully used as the counteranion/dopant for electrosynthesis of conducting polymers, for example, polypyrrole and polyaniline.[8−12] However, no attempt has yet been made to use the anionic CNTs as the supporting electrolyte for the electrosynthesis of nonconducting polymers. Here we explore a novel concept of using an aqueous suspension of acid-treated CNTs to mitigate the above-mentioned self-limiting problem in the electropolymerization process by weakening the insulating barrier on the electrode surface. In this work, two nonconducting polymers were investigated, namely poly(*o*-aminophenol) (P*o*AP) and poly(*m*-phenylenediamine) (P*m*PD).[4,13−20] Since the synthesis process and the product morphology of these two polymers are quite similar, the discussion below will focus on results related with P*o*AP. The mechanism behind this approach and the promising applications of the synthesized P*o*AP−CNT composite will be discussed and investigated. The findings may provide a new research direction for the making and applications of CNTs and nonconducting polymer composites.

RESULTS AND DISCUSSION

Electro-co-deposition. Electro-co-deposition of P*o*AP and CNTs was first carried out by potentiodynamic polymerization of 10 mL of solution of *o*AP (monomer, 10 mmol L^{-1}) in an aqueous suspension of acid-treated multiwalled CNTs (0.2 wt %) without any other electrolyte. For comparison, pure P*o*AP films were electropolymerized under the same condition but in 0.5 mol L^{-1} KCl aqueous solution. Figure 1a presents the cyclic voltammograms (CVs) of polymerization of *o*AP in KCl solution.

It was found that the currents recorded through the forward potential scan were

*Address correspondence to george.chen@nottingham.ac.uk.

Received for review April 22, 2010 and accepted June 8, 2010.

Published online June 15, 2010. 10.1021/nn100849d

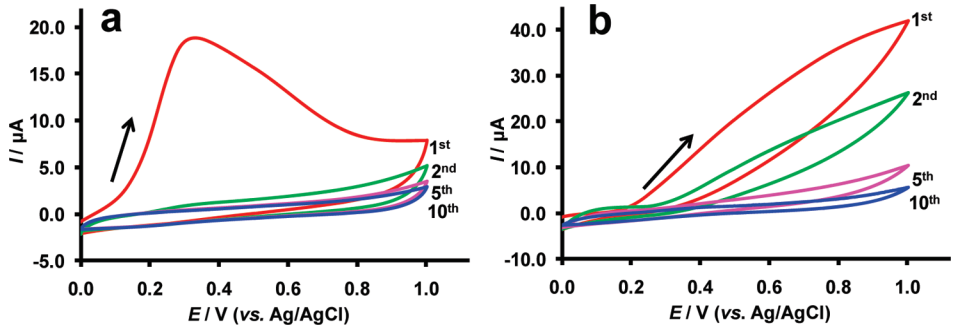

Figure 1. Potentiodynamic polymerization of 10 mmol L^{-1} *o*AP in (a) 0.5 mol L^{-1} KCl aqueous solution and (b) 0.2 wt % CNT aqueous suspension. Numerals indicate the number of potential cycles. Arrows show the direction of potential scan. Scan rate: 20 mV s^{-1}.

larger than those at the same potentials during the backward potential scan. These current attenuations together with the light brown coating on the working electrode (Pt disk electrode, 1.6 mm in diameter, the same electrode below) imply that a nonconducting polymer film was formed on the electrode surface.

In addition, Figure 1a shows a high anodic current peak at around 0.35 V *vs* Ag/AgCl during the first potential cycle, which can be attributed to the oxidation of the monomer. However, in the CNT suspension with the same monomer concentration, the currents were much larger, and there was no peak on the first cycle CV as shown in Figure 1b. From the second cycle, the currents decreased sharply in Figure 1a, but to a much smaller degree in Figure 1b. These differences can be rationalized by considering that there were differences in the electrolyte composition, particularly the counterions (Cl^- *vs* anionic CNTs), and also competition between the electrode potential increase and the resistance increase in the case of P*o*AP. On the first cycle CV in Figure 1a, the current initially rose with the electrode potential increase, and then dropped after the peak, which was likely related to the depletion of the reactant near the electrode surface (diffusion-controlled process). However, the trend of the current decline after the peak was quite different from that due to solely diffusion control, suggesting an additional effect. It could be the newly formed nonconducting film becoming too resistive to allow further formation of the nonconducting polymer (self-limiting). This in turn retarded the growth of the polymer film (further resistance increase), resulting in the current declining to a fairly low current plateau (at around 0.85 V, Figure 1a). During the successive potential cycles, the anodic current peak disappeared because the electrode surface had been covered with a sufficiently resistive film. Interestingly, the anodic current peak was completely absent during electro-co-deposition of P*o*AP and CNTs in the aqueous suspension of CNTs (Figure 1b), which can be attributed to the high specific surface area and good electronic conductivity of the CNTs. The high specific surface area of CNTs can enlarge the real electrode surface area (increasing current) which is capable of canceling the diffusion-controlled effect (decreasing current). Additionally, under the same electropolymerization charge, the quantity of synthesized nonconducting polymer on the original electrode surface should be equal to that on CNTs. Because of the high specific surface area of the CNTs, the coating thickness of nonconducting polymer on individual nanotube surfaces can be significantly reduced, diminishing the electron transfer barrier (the resistance) on the electrode and leading to the continuously increasing current. These were evidenced by the differences between the CVs in Figure 1 panels a and b: (a) the continuously increasing current without any peak in the first potential cycle of Figure 1b and (b) the significantly higher currents in the following potential cycles in Figure 1b compared to those in Figure 1a.

For further investigation, potentiostatic polymerization was carried out in the same solutions. On the basis of the observed anodic current peaks in Figure 1a, a constant potential of 0.35 V *vs* Ag/AgCl was chosen to ensure the occurrence of electropolymerization while avoiding overoxidation.[12] During potentiostatic polymerization, the current−time curve, as shown in Figure 2, kept decreasing over time, which indicates the formation of a nonconducting polymer film on the electrode. Initially, the electro-co-deposition current in the aqueous suspension of CNTs was lower than that in the KCl solution. This can be ascribed to the inferior mobility of the anionic CNTs which served as macro-charge-

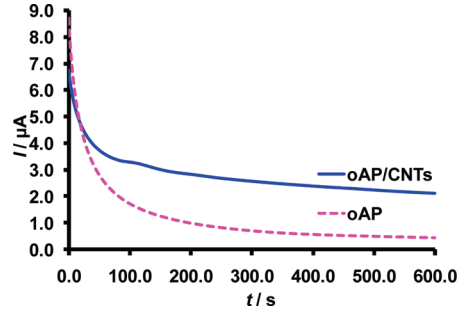

Figure 2. Potentiostatic polymerization of 10 mmol L^{-1} *o*AP in (a) 0.5 mol L^{-1} KCl aqueous solution (dashed line) and (b) 0.2 wt % CNT aqueous suspension (solid line). Electrode potential: 0.35 V. Reference electrode: Ag/AgCl (3.0 mol L^{-1} KCl aqueous solution).

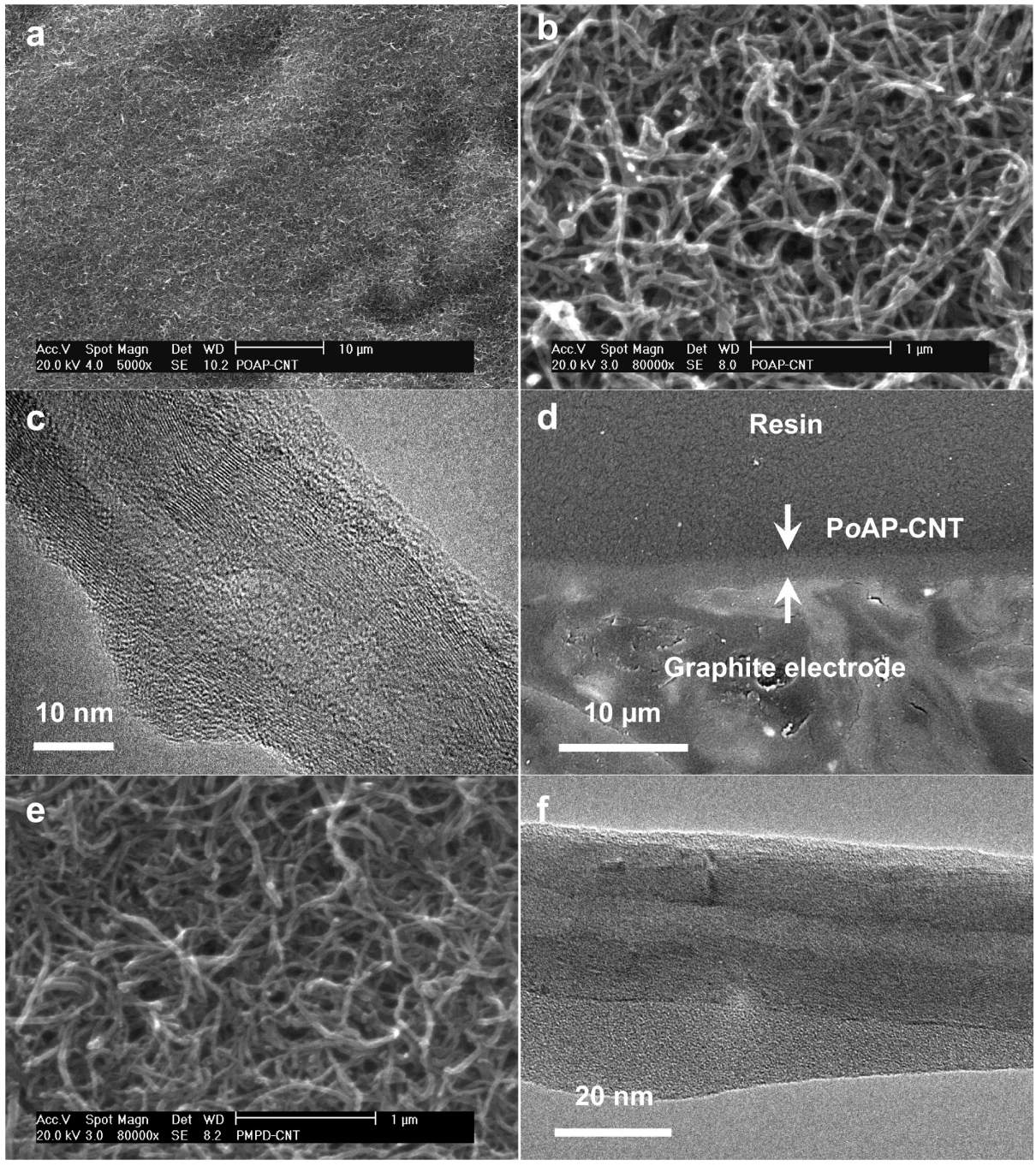

Figure 3. SEM images of (a) PoAP−CNT composite film, (b) porous structure of PoAP−CNT composite film; (c) TEM image of PoAP-coated CNT; (d) BSE−SEM image of a cross-section of a PoAP−CNT covered electrode; (e) porous structure of PmPD−CNT composite film; (f) TEM image of PmPD-coated CNT. All samples were prepared as described in Figure 1.

carriers during the electropolymerization process and hence resulted in a lower conductivity of the CNT suspension compared to that of the KCl solution.[12] Nevertheless, coupled with the extended progression of the self-limiting electropolymerization, the merits of using this novel CNT electrolyte is clearly evident by the cross point of the two current−time curves located at approximately the 18th second. Beyond this point, the current for electro-co-deposition of PoAP−CNT started to remain at a higher value than that for electrodeposition of PoAP with final current values at 600 s of 2.13 μA for PoAP−CNT and 0.43 μA for PoAP. This higher current during potentiostatic polymerization implies that the presence of CNTs in nonconducting polymer matrixes considerably enhances the electronic conductivity of the coating.

Electron Microscopy. Further evidence supporting the proposed mechanism was exhibited by scanning electron microscopy (SEM). Under SEM, a uniform and continuous PoAP−CNT composite film was observed on the surface of the electrode (Figure 3a). High-resolution SEM indicated that the PoAP−CNT composite films

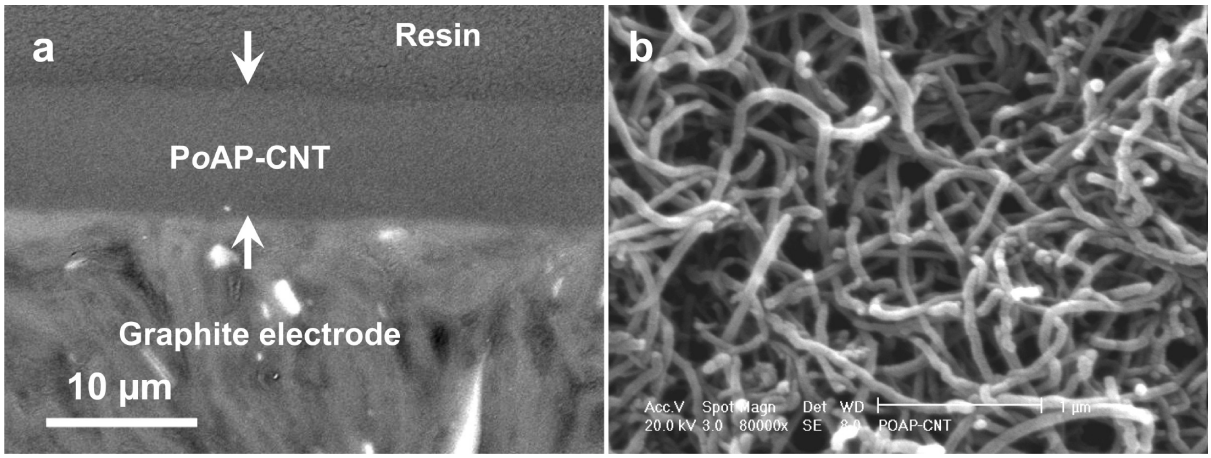

Figure 4. (a) BSE-SEM image of the cross-section of a PoAP−CNT covered electrode; (b) SEM image of porous structure of PoAP−CNT composite film. All samples presented were electro-co-deposited from solutions containing 50 mmol L^{-1} monomer and 0.2 wt % CNTs by sweeping the potential 10 times in the range of 0−1.0 V. Scan rate: 20 mV s^{-1}.

were extremely porous, forming a three-dimensional (3D) network consisting of interconnected fibrils with similar diameters (Figure 3b). The diameter of the acid-treated CNTs is in the range of 10−50 nm, while that of the fibrils in the composite is in the range of 20−60 nm, indicating that the PoAP formed an ultrathin coating layer on the surface of individual CNTs. Obviously, the 3D network of coated CNTs and the micro- and nanopores between them as seen in Figure 3b can provide sufficient pathways for electron conduction and also for the movement of monomers within the film and therefore temper the self-limiting barrier effect to continuous deposition of the nonconducting polymer.

The SEM observations stimulated curiosity as to how the PoAP coatings were formed on the surface of individual CNTs. Thus, high-resolution transmission electron microscopy (HRTEM) was used to investigate the PoAP−CNT composites. Under HRTEM (Figure 3c), the coated nanotubes exhibit both the central cavity and an amorphous coating. Between them are the graphitic fringes of the nanotube. As the disturbance dimension on the outer surface of CNTs examined after acid treatment was less than 1 nm,[10] the amorphous thin coating (1.5−6.0 nm in thickness) can only be attributed to PoAP. This is different from the conducting polymer coating where the covering thickness on individual nanotubes could reach beyond 100 nm.[10] This uneven and ultrathin coating layer outside the nanotube strongly confirms the previously proposed mechanism derived from the CVs.

The thickness of PoAP−CNT composite was additionally revealed by back scattered electron imaging (BSE)-SEM. In Figure 3d, the observed thickness of the PoAP−CNT film is in the range of 2.3−3.6 μm. On the contrary, the presence of the pure PoAP film (possibly less than 100 nm in thickness) was just vaguely visible on the electrode surface, but it was challenging to quantify the film's thickness as the scanning electron microscope was at its resolution limit under the BSE conditions. Since the film thickness of PoAP is self-controlled or self-limited during the electropolymerization, the thickness of the PoAP film formed here should not be more than a few tens of nanometers. Indeed, according to the literature, the electrodeposited pure PoAP film was estimated to be in the range of 57−65 nm.[13] The significant increase in thickness of the composite film can be attributed to the entrapped CNTs in the nonconducting PoAP which can provide extra electron pathways and new reaction (deposition) sites among the insulating matrix for further electropolymerization, leading to a much thicker composite film. The SEM and TEM images of the PmPD−CNT composite films synthesized under the same condition are shown in Figure 3e,f, further confirming the feasibility and universality of this novel approach.

It is interesting to see if the concentration of the monomer may affect the process and product of electro-co-deposition. As shown in Figure 4a, under the same conditions except for a higher monomer concentration (oAP, 50 mmol L^{-1}), the thickness of the deposited PoAP−CNT film is in the range of 7.4−8.2 μm, which is about 3 times thicker than the 2.3−3.6 μm composite film presented in Figure 3d.

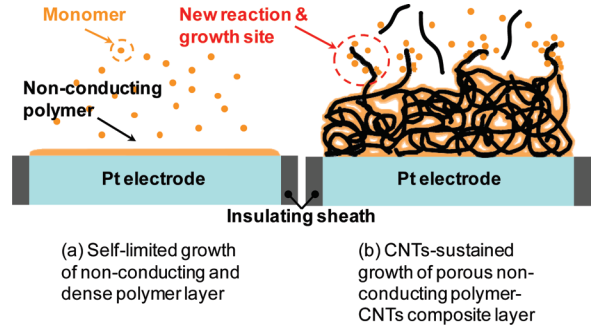

Figure 5. Schematic diagrams of the electrode covered with (a) a pure nonconducting polymer layer and (b) a nonconducting polymer−CNT composite layer on which the interconnected CNTs represent the electrode sites where further electropolymerization occurs.

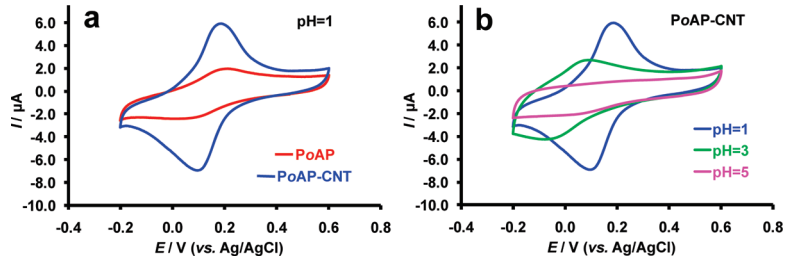

Figure 6. Cyclic voltammograms of (a) PoAP (red line) and PoAP−CNT (blue line) modified Pt electrodes in HCl solution at pH =1.0, and (b) PoAP−CNT-modified Pt electrode at different pH values of 1.0, 3.0, and 5.0 in HCl solution. Scan rate: 10 mV s^{-1}. The modified electrodes were prepared in 50 mmol L^{-1} monomer (oAP) solutions containing 0.5 mol L^{-1} KCl or 0.2 wt % CNTs by sweeping the potential 10 times between 0 and 1.0 V. Scan rate: 20 mV s^{-1}.

However, as expected, Figure 4b reveals a very similar 3D network and the consequent porous structure in this thicker composite film, although the PoAP-coated CNTs are notably thicker (50−100 nm) than those (20−60 nm) exhibited in Figure 3b,e. Thus, to grow thicker coatings on individual CNTs, it would be preferable to use high monomer concentrations to obtain thicker composite layers on the electrode, and polymer layers on nanotubes. Based on the aforementioned findings and discussion, Figure 5 depicts the role of CNTs in the self-limiting electropolymerization process.

Potential Applications. As shown in Figure 3 and 4, the thin PoAP (or PmDP) layers on individual CNTs can help entrap ionic or molecular species that are interactive with the nonconducting polymer. Since the entrapped species are in close proximity to the CNT networks that connect to the transducer surface, a faster response time is anticipated. Moreover, due to the much thicker composite film, the total amount of entrapped species should dramatically increase.

The fabrication of an amperometric glucose biosensor based on PoAP−CNT through electro-deposition in solutions containing additional supporting electrolytes was reported previously.[14] On the basis of SEM findings, the anions of the supporting electrolyte, such as CH_3COO^- and Cl^- that participated in the electropolymerization process, may cause polymer agglomeration and the formation of a less porous structure compared to those seen in Figures 3b,e and 4b.[14] On the other hand, most previous studies on PoAP or PoAP−CNT are focused on using them as a matrix or immobilizer to entrap functional molecules for sensor applications,[13−18] but little is reported on exploitation of the electrochemical properties of PoAP or PoAP−CNT. It is known that the solution pH can influence the electrochemical activity of PoAP which is electro-active in acidic solutions but become inactive when the pH approaches 7.[19]

In this work, the electrochemical responses of the electro-deposited PoAP and PoAP−CNT composite films were first measured in HCl solutions at pH values of 1.0, 3.0, and 5.0. Figure 6a presents the CVs recorded at pH = 1.0 on the PoAP and PoAP−CNT-modified Pt electrodes. The reduction and oxidation current peaks can be observed here, indicating the occurrence of ion doping and dedoping,[19] which will be further discussed later. Moreover, it can be seen clearly that the PoAP−CNT-modified electrode exported much larger current peaks than the pure PoAP-modified electrode, showing a greater electro-activity toward protons. This phenomenon can be explained by the composite having significantly increased porosity and hence larger polymer/electrolyte interfacial area, and also enhanced electronic and ionic conductivities through the interconnected CNTs and the pores between them.[10−12] When the solution pH was raised to 3.0 or 5.0, as shown in Figure 6b, both the oxidation and reduction peak currents decreased, accompanied by negative shifts of the current peak potentials. This can be explained by the degree of protonation of the imino groups in PoAP decreasing with lowering the solution acidity, and hence the redox activity.[19,20] The electro-activity of PoAP in response to protonation as reported in the literature[21] is summarized in Scheme 1

The high sensitivity of the PoAP−CNT composite to pH variation stimulated a thought of using it for sensing CO_2 whose dissolution in water lowers the pH. In the preliminary tests, the PoAP and PoAP−CNT modified Pt electrodes were prepared by potentiodynamic depo-

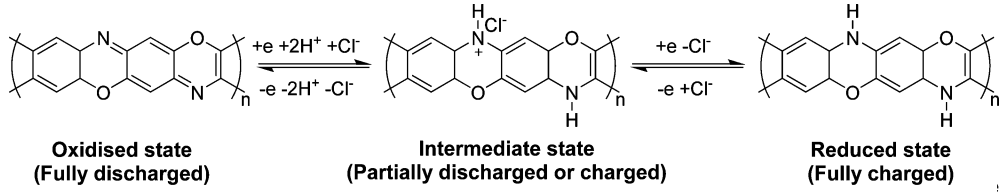

Scheme 1. Pathway for the redox chemistry of PoAP in the HCl solution.[21] Indications of charged and discharged states are with reference to using the polymer as the negative electrode material in a supercapattery as discussed in the text and illustrated in Figure 8.

sition in 50 mmol L^{-1} monomer solutions to gain larger polymer/electrolyte interfacial area. After electrodeposition, the electrode was rinsed in water and then transferred to the 3 mol L^{-1} KCl aqueous solution which was predeaerated by argon. Then, the open circuit potential (OCP) of the modified Pt electrode was recorded before and after bubbling the CO_2 gas (flow rate = 6 mL min^{-1}) into the solution. In the CO_2 bubbling experiment, it was found that the pH of the neutral solution usually reached, and then stabilized at, about 4 within 10 min.

In the experiments it was observed that, before CO_2 bubbling, the OCP of either of the two electrodes always varied with the immersion time, but the variations were inconsistent between experiments. The two OCP-time plots in Figure 7 were selected to show the opposite OCP shifts of the two electrodes, although variations in the same direction were also observed. In general, the shift of the OCP with time indicates interactions, particularly ion exchanges, between the P*o*AP or P*o*AP−CNT film and the 3 mol L^{-1} KCl solution. For example, the electrodeposition of either P*o*AP or P*o*AP−CNT was carried out in solutions containing less or no KCl. Also, the obtained deposits were manually rinsed in water before OCP recording. This operation was to remove the remaining solution phase species in the deposits, such as monomers and loose CNTs or the supporting electrolyte, that is, KCl. However, after this manual work, the state of the P*o*AP or P*o*AP−CNT deposit could vary between different experiments, which may account for the observed inconsistency of the OCP variation.

CO_2 bubbling was started after the OCP became relatively stable, and the OCP values of the two electrodes always increased positively and fairly quickly reached a plateau. Interestingly, as can be seen in Figure 7, the OCP of the P*o*AP−CNT film increased by a larger value (40 mV) than that of the P*o*AP (20 mV). This could be attributed to the P*o*AP and the anionic CNTs in the composite both being capable of responding to the pH change in the solution resulting from CO_2 bubbling. While further research is ongoing in this laboratory, this preliminary finding promises an application of the P*o*AP−CNT film for CO_2 sensing.

There are many redox active polymers, but very few are reducible, particularly in aqueous solutions.[10−12,22−25] For example, polyaniline (PANi) is a well-studied conducting polymer capable of undergoing fairly reversible multistep oxidation in acidic media.[12] Particularly, it was reported that the theoretical specific capacitance of PANi could be as high as 750 F/g.[22] It is also possible to prepare PANi−CNT composites by chemical[22,23] or electrochemical[12,24] methods to gain enhanced performance in terms of discharging and charging speed and cycling stability. Unfortunately, PANi shows only satisfactory capacitive behavior in a quite narrow range of positive potentials (0.1−0.7 V)[12]

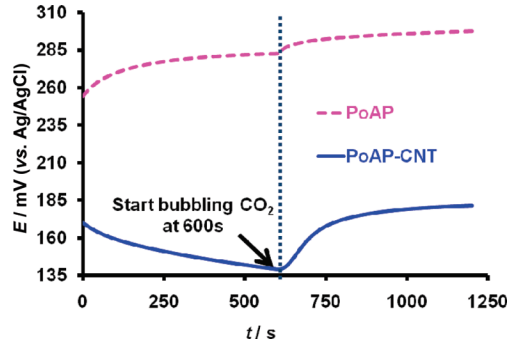

Figure 7. Variation of OCP of (a) P*o*AP (dashed line) and (b) P*o*AP−CNT (solid line) modified Pt electrodes in 3 mol L^{-1} KCl before (≤600 s) and after (>600 s) CO_2 bubbling (6 mL min^{-1}).

which is unfavorable for using PANi as both positive and negative electrodes in the so-called symmetrical electrochemical capacitors (supercapacitors). The CVs presented in Figure 6 suggest P*o*AP−CNT to be a suitable complement to PANi−CNT in terms of potential range. It should be noted that PANi−CNT stores charge through its pseudocapacitance (featured by rectangular CVs), while P*o*AP−CNT does so in the usual Faradic manner (showing peak shaped CVs). Thus, the use of P*o*AP−CNT and PANi−CNT as the negative and positive electrode materials, respectively, in the same cell would lead to a hybrid energy storage device that truly is a supercapattery. (The term "capattery" was previously used for supercapacitors, but received academic objections.[25,26]) It is worth pointing out that PANi becomes nonconducting in the neutral or discharged (reduced) state. Thus, the presence of CNTs in PANi can help overcome this problem by maintaining conductivity.[10−12,24] This role of CNTs is particularly important for P*o*AP which is non- or poorly conducting in both fully charged (reduced) and discharged (oxidized) states. On the other hand, like PANi, the redox chemistry of P*o*AP involves both protons and anions (Cl^- in the HCl solution), as explained in **Scheme 1**. This common feature between PANi and P*o*AP, together with the contribution of CNTs to conductivity, makes them an ideal pair to work in a supercapattery with acidic electrolytes.

For verification, the P*o*AP−CNT and PANi−CNT composites were each electro-deposited on the Pt disk electrode (1.6 mm in diameter) for recording CVs, or on relatively larger graphite disk electrodes (6.0 mm in diameter) for construction of laboratory supercapacitors and supercapatteries. The PANi−CNT composite was prepared, as previously repored,[12,24] by potentiostatic deposition at 0.9 V in a solution of 1.0 mol L^{-1} HCl, 0.25 mol L^{-1} aniline, and 0.2 wt % CNTs. In the electrodeposition of both composites, the charge was controlled to be the same for comparison.

Figure 8a superimposes the CVs of both P*o*AP−CNT and PANi−CNT in 1.0 mol L^{-1} HCl. It can be seen that the potential ranges for the two composites to remain electro-active are fairly different, with P*o*AP−CNT in the

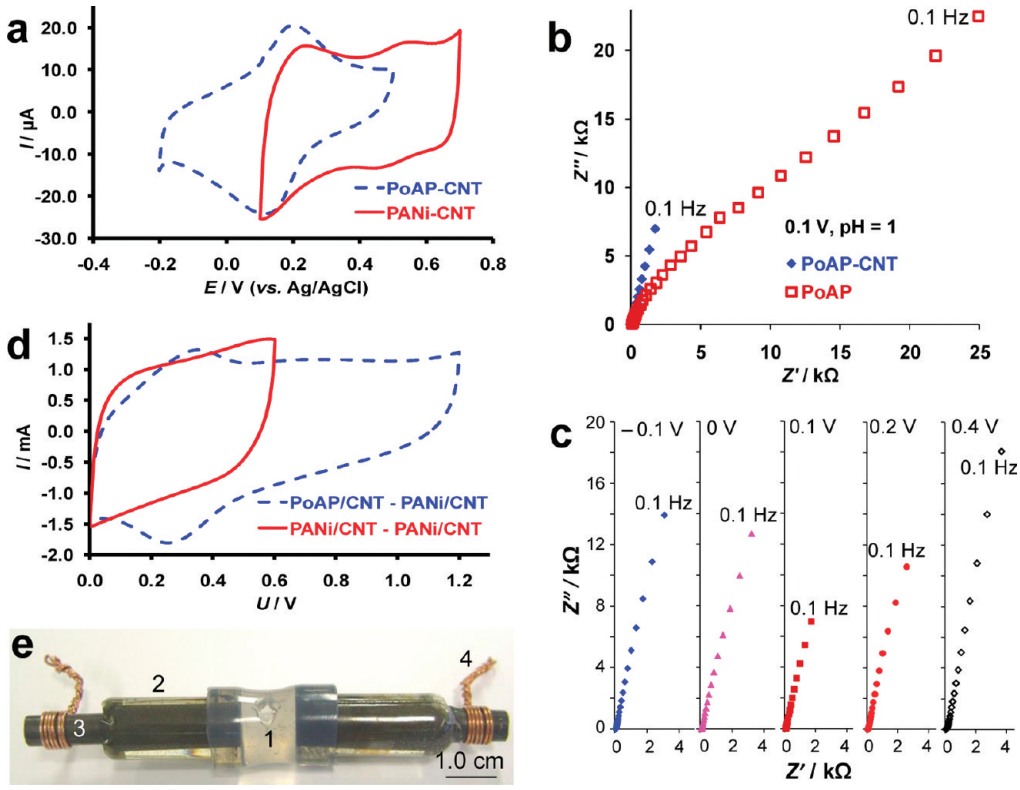

Figure 8. (a) CVs of PANi−CNT (red solid line) and PoAP−CNT (blue dashed line) modified Pt disk electrodes (1.6 mm diameter) in 1.0 mol L^{-1} HCl solution. Scan rate: 50 mV s^{-1}. Deposition charge on each electrode was 1.2 mC. (b,c) Nyquist impedance plots of (b) PoAP−CNT (filled diamonds) and PoAP (empty squares) at 0.1 V in HCl solution (pH = 1) and (c) PoAP−CNT at different potentials. Deposition charge: 1.1 mC. (d) CVs of the symmetrical supercapacitor of PANi−CNT (±) | HCl (1.0 mol L^{-1}) | PANi−CNT (∓) (red solid line), and the supercapattery of PANi−CNT (+) | HCl (1.0 mol L^{-1}) | PoAP−CNT (−) (blue dashed line), scan rate 200 mV s^{-1}. Deposition charge on each electrode was 64 mC. (e) Photo of the tube cell used for recording the CVs in panel d: (1) silicone rubber tube with a hole for electrolyte addition, (2) epoxy resin sheath, (3) graphite rod, (4) copper wire.

−0.20 to 0.50 V range and PANi−CNT in the 0.10−0.7 V range. Also, the total charge enclosed in the CV of PANi−CNT is larger than that of PoAP−CNT, although the former was tested in a narrower potential range. These CVs confirm PANi−CNT to be indeed a high capacity charge storage material at positive potentials, while PoAP−CNT is suitable as a negative electrode material for pairing with PANi−CNT.

For electrochemical energy storage, the electronic and ionic conductivities of the electrode materials need to be sufficiently high. The PANi−CNT composite was reported before to be highly conductive,[12,24] but no such information is available in the literature for the PoAP−CNT composite. Figure 8b compares the Nyquist impedance plot of the PoAP−CNT film on the Pt disk electrode at 0.1 V in the HCl solution (pH = 1). For comparison, the Nyquist impedance plot of the PoAP film prepared under the same conditions are also presented. In an early study, the low frequency impedance data were used to derive the conductivity of electrodeposited PoAP films at different potentials.[27] It was reported that the conductivity of PoAP depended strongly on the potential with a maximum of $4.55 \pm 0.2 \times 10^{-7}$ S cm^{-1} at the equilibrium potential which is *ca.* 0.15 V *vs* Ag/AgCl according to Figure 6. At other potentials, the conductivity dropped significantly. As shown in Figure 8b, the PoAP−CNT film had much lower impedance than the PoAP film. For example, at 0.1 Hz, the real component of the impedance was 24.9 kΩ for the PoAP film and 1.73 kΩ for the PoAP−CNT film, suggesting an increase of *ca.*15-fold in conductivity. This difference reflects very well the contribution of the highly conducting CNTs to electron transport through the electro-deposited composite film.

It is worth pointing out that the ac impedance of PoAP−CNT was also dependent on the potential, as shown in Figure 8c. However, in comparison with PoAP,[27] the variation was much less dramatic and the changes were more on the imaginary component. Particularly, at all applied potentials, the Nyquist plots of PoAP−CNT were dominated by the capacitive feature (a tilted vertical line) and showed no sign of a charge transfer barrier (*i.e.*, a semicircle at high frequencies). These findings reflect again the roles of the interconnected CNTs in provision of effective pathways for electrons along the CNTs and for ions through the pores between the CNTs (*cf.* Figures 3b and 4b). Thus, the ac impedance study provides further justification for pairing PoAP−CNT with PANi−CNT in the proposed supercapattery.

The composites deposited on the 6 mm graphite disks were combined into a tube-type laboratory cell, using PANi−CNT and P*o*AP−CNT as the positive and negative electrode materials, respectively. Figure 8d presents the CVs from the tube cell whose photograph is given in Figure 8e. It can be clearly seen that the PANi−CNT (+) | HCl (1.0 mol L^{-1}) | P*o*AP−CNT (−) cell, or supercapattery, exhibits both peaks (0.2−0.4 V) and capacitive currents (0.5−1.2 V). The working voltage of the supercapattery could reach 1.2 V, which compares favorably with the voltage range of 0.6 V exhibited by a similarly built symmetrical supercapacitor of PANi−CNT (±)| HCl (1.0 mol L^{-1}) | PANi−CNT (∓). This improvement in cell voltage can be attributed to the electrochemical activity of P*o*AP−CNT at negative potentials. Note that the cell shown in Figure 8e is completely free of metal (except for the external wiring).

SUMMARY

We have explored a novel approach to electro-co-deposition of CNTs and nonconducting polymers, namely P*o*AP and P*m*DP, into fairly thick, porous, and conducting composite films. In this process, the self-limiting growth of the nonconducting polymer is mitigated by using an aqueous suspension of acid-treated CNTs as the only supporting electrolyte. The mechanism behind this approach is that the CNTs serve as the anionic charge carriers in the liquid phase during electro-co-deposition and the backbone of the porous structure within the composite films. More importantly, during electro-co-deposition, the dispersed CNTs in the nonconducting polymer provide electron pathways and new reaction sites for continuous electropolymerization which would otherwise have ceased after the full coverage of the electrode surface by the nonconducting polymer.

In the electro-co-deposited composite films, the CNTs are individually coated by a thin layer of the nonconducting polymer and interconnected into a highly porous 3D network. These features are beneficial to both electronic and ionic conductions through the CNTs and the pores between them, respectively, and also to the interactions between the polymer and a substrate in solution. These properties promise applications as preliminarily demonstrated by using the P*o*AP−CNT composite as the electro-sensing material for detection of pH changes in water that may result from CO_2 dissolution, or as the negative electrode material in an unprecedented laboratory supercapattery of PANi−CNT (+) | HCl (1.0 mol L^{-1}) | P*o*AP−CNT (−) that works in a much wider voltage range than the similarly constructed symmetrical supercapacitor of PANi−CNT (±) | HCl (1.0 mol L^{-1}) | PANi−CNT (∓).

Overall, in our view, this paper has consolidated the feasibility of electro-co-deposition for making composites of nonconducting polymers and CNTs. The reported preliminary findings on potential applications of these composites in chemical sensing and charge storage highlight a new direction of research toward more redox active and nanostructured functional materials, including those of biological significance.[5,6,13−18]

EXPERIMENTAL SECTION

For electrochemical measurements in the three-electrode cell, a platinum (Pt) disk (1.6 mm in diameter) was used as the working electrode. The counter-electrode was a 6.0 mm diameter graphite rod. An Ag/AgCl half-cell containing an aqueous solution of 3.0 mol L^{-1} KCl was applied as the reference electrode in all electrochemical experiments. The 6.0 mm diameter graphite rod was also used to make a disk electrode by sheathing the side wall of the rod with a 5−6 mm thick layer of epoxy resin. After electro-co-deposition, the end of the graphite rod with the deposit was cut off and mounted on an SEM sample holder for morphological analysis. For film thickness observation, the graphite rod with the deposited film was first immersed in resin. After hardening for 24 h, the sample was ground on sand paper and then polished using alumina paste to expose the cross-section of the deposited film. For TEM examinations, polymer composites were first dispread in acetone by ultrasonication, and then loaded on the holey carbon-film-coated copper grid. Deionized water was used for preparing solutions and rinsing electrodes. Reagents of *o*-aminophenol (99+%, Fluka), *m*-phenylenediamine (98+%, Fluka), aniline (99.5+%, Aldrich), KCl (99%, Sigma), and HCl (37% in water, Acros) were used as supplied.

Multiwalled CNTs (Shenzhen Nanotech Port Co., Ltd.) were boiled in a mixture of concentrated sulfuric and nitric acids (3:1 v/v) for about 30 min. After cooling to room temperature, the suspension was bath sonicated for 10 min, and then filtered and washed in water to pH 6−7. The obtained acid-treated CNTs were further diluted to form a suspension containing 0.2 wt % CNTs.

The electro-co-deposition process was carried out in 10 mL aqueous solution of the monomer (10 or 50 mmol L^{-1}) and acid-treated CNTs. For comparison, pure polymer was electrodeposited from an aqueous solution containing a given monomer (10 or 50 mmol L^{-1}) and KCl (0.5 mol L^{-1}). Potentiodynamic polymerization was carried out by cycling the potential in the range of 0.0−1.0 V at a scan rate of 20 mV s^{-1} against the Ag/AgCl reference electrode. Potentiostatic polymerization was typically carried out at a given potential for a designated deposition time or charge.

The electro-deposited films on the Pt disk electrode were studied by cyclic voltammetry and ac impedance (0.1 Hz~100 kHz) in a three-electrode cell (10 mL) containing aqueous HCl solutions at different pH with or without added KCl to maintain the electrolyte strength. Open circuit potential measurements of the electro-deposited films were also carried out in the 3 mol L^{-1} KCl solution, with or without CO_2 bubbling at a flow rate of 6 mL min^{-1}.

A tube-type two-electrode cell was built using two graphite disk electrodes that were predeposited with the desired polymer−CNT composites. The two electrodes were forced into each end of a silicone rubber tube with an inner diameter of 10 mm. A small hole was cut in the tube wall between the two electrodes to allow electrolyte (1.0 mol L^{-1} HCl) injection using a pipet. The distance between the surfaces of the two electrodes was 10 mm. Thus, the amount of electrolyte was calculated as *ca.* 0.8 mL.

The PGSTAT30 Autolab Potentiostat (EcoChemie, Inc.) was used for all electrochemical controls. The microstructures and morphologies of the samples were investigated on a Philips XL30 FEG (SEM), Quanta 600 ESEM (BSE-SEM), and HRTEM JEOL-2100F (TEM).

Acknowledgment. We thank E.ON AG for the International Research Award (Energy Storage, 2007). Responsibility for the content of this publication lies with the authors.

REFERENCES AND NOTES

1. Miao, Y.; Chen, J.; Wu, X. Using Electropolymerized Nonconducting Polymers to Develop Enzyme Amperometric Biosensors. *Trends Biotechnol.* **2004**, *22*, 227–231.
2. Snook, G. A.; Peng, C.; Fray, D. J.; Chen, G. Z. Achieving High Electrode Specific Capacitance with Materials of Low Mass Specific Capacitance: Potentiostatically Grown Thick Micro-Nanoporous PEDOT Films. *Electrochem. Commun.* **2007**, *9*, 83–88.
3. Park, J. K.; Tran, P. H.; Chao, J. K. T.; Ghodadra, R.; Rangarajan, R.; N, V. T. *In Vivo* Nitric Oxide Sensor using Nonconducting Polymer-Modified Carbon Giber. *Biosens. Bioelectron.* **1998**, *13*, 1187–1195.
4. Xu, J.; Sun, X.; Liu, B.; Xu, F. Poly-*m*-phenylenediamine Modified Electrode as a pH Sensor. *Anal. Sci.* **2001**, *17*, i1363.
5. Malitesta, C.; Palmisano, F.; Torsi, L.; Zambonin, P. G. Glucose Fast-Response Amperometric Sensor Based on Glucose Oxidase Immobilized in an Electropolymerized Poly(*o*-phenylenediamine) Film. *Anal. Chem.* **1990**, *62*, 2735–2740.
6. Myler, S.; Eaton, S.; Higson, S. P. J. Poly(*o*-phenylenediamine) Ultra-Thin Polymer-Film Composite Membranes for Enzyme Electrodes. *Anal. Chim. Acta* **1997**, *357*, 55–61.
7. Chung, T. D.; Jeong, R.-A.; Kang, S. K.; Kim, H. C. Reproducible Fabrication of Miniaturized Glucose Sensors: Preparation of Sensing Membranes for Continuous Monitoring. *Biosens. Bioelectron.* **2001**, *16*, 1079–1087.
8. Li, C.; Bai, H.; Shi, G. Q. Conducting Polymer Nanomaterials: Electrosynthesis and Applications. *Chem. Soc. Rev.* **2009**, *38*, 2397–2409.
9. Su, D. S.; Schloegl, R. Nanostructured Carbon and Carbon Nanocomposites for Electrochemical Energy Storage Applications. *ChemSusChem* **2010**, *3*, 136–168.
10. Chen, G. Z.; Shaffer, M. S. P.; Dan, C.; Dixon, G.; Zhou, W.; Fray, D. J.; Windle, A. H. Carbon Nanotube and Polypyrrole Composites: Coating and Doping. *Adv. Mater.* **2000**, *12*, 522–526.
11. Peng, C.; Snook, G. A.; Fray, D. J.; Shaffer, M. S. P.; Chen, G. Z. Carbon Nanotube Stabilized Emulsions for Electrochemical Synthesis of Porous Nanocomposite Coatings of Poly[3,4-ethylene-dioxythiophene]. *Chem. Commun.* **2006**, 4629–4631.
12. Peng, C.; Jin, J.; Chen, G. Z. A Comparative Study on Electrochemical Co-deposition and Capacitance of Composite Films of Conducting Polymers and Carbon Nanotubes. *Electrochim. Acta* **2007**, *53*, 525–537.
13. Guerrieri, A.; Ciriello, R.; Centonze, D. Permselective and Enzyme-Entrapping Behaviours of an Electropolymerized, Nonconducting, Poly(*o*-aminophenol) Thin Film-Modified Electrode: A Critical Study. *Biosens. Bioelectron.* **2009**, *24*, 1550–1556.
14. Pan, D.; Chen, J.; Yao, S.; Tao, W.; Nie, L. An Amperometric Glucose Biosensor Based on Glucose Oxidase Immobilized in Electropolymerized Poly(*o*-aminophenol) and Carbon Nanotubes Composite Film on a Gold Electrode. *Anal. Sci.* **2005**, *21*, 367–371.
15. Abdel-Hamid, I.; Atanasov, P.; Wilkins, E. Development of a Needle-Type Biosensor for Intravascular Glucose Monitoring. *Anal. Chim. Acta* **1995**, *313*, 45–54.
16. Zhang, Z.; Liu, H.; Deng, J. A Glucose Biosensor Based on Immobilization of Glucose Oxidase in Electropolymerized *o*-Aminophenol Film on Platinized Glassy Carbon Electrode. *Anal. Chem.* **1996**, *68*, 1632–1638.
17. Pan, D.; Chen, J.; Nie, L.; Tao, W.; Yao, S. Amperometric Glucose Biosensor Based on Immobilization of Glucose Oxidase in Electropolymerized *o*-Aminophenol Film at Prussian Blue-Modified Platinum Electrode. *Electrochim. Acta* **2004**, *49*, 795–801.
18. Li, J.; Lin, X. Glucose Biosensor Based on Immobilization of Glucose Oxidase in Poly(*o*-aminophenol) Film on Polypyrrole−Pt Nanocomposite Modified Glassy Carbon Electrode. *Biosens. Bioelectron.* **2007**, *22*, 2898–2905.
19. Zhang, Y.-Y.; Wang, M.-L.; Liu, M.-L.; Yang, Q.; Xie, Q.-J.; Yao, S.-Z. Growth and Properties of Poly-*o*-aminophenol Films with Three Dimensional Combinations of *in Situ* Electrochemical Quartz Crystal Microbalance and Fourier Transform Infrared Spectroelectrochemistry. *Chin. J. Anal. Chim.* **2007**, *35*, 685–690.
20. Tucceri, R. I. Specularity Change on a Thin Gold Film Surface Coated with Poly(*o*-aminophenol) during the Polymer Redox Conversion. The pH Effect on the Redox Sites Distribution at the Metal|Polymer Interface. *J. Electroanal. Chem.* **2003**, *543*, 61–71.
21. Salavagione, H. J.; Arias-Pardilla, J.; Pérez, J. M.; Vázquez, J. L.; Morallón, E.; Miras, M. C.; Barbero, C. Study of Redox Mechanism of Poly(*o*-aminophenol) using *in Situ* Techniques: Evidence of Two Redox Processes. *J. Electroanal. Chem.* **2005**, *576*, 139–145.
22. Lota, K.; Khomenko, V. K.; Frackowiak, E. Capacitance Properties of Poly(3,4-ethylenedioxythiophene)/Carbon Nanotubes Composites. *J. Phys. Chem. Solids* **2004**, *65*, 295–301.
23. Frackowiak, E.; Khomenko, V.; Jurewicz, K.; Lota, K.; Beguin, F. Supercapacitors Based on Conducting Polymers/Nanotubes Composites. *J. Power Sources* **2006**, *153*, 413–418.
24. Wu, M. Q.; Snook, G. A.; Gupta, V.; Shaffer, M; Fray, D. J.; Chen, G. Z. Electrochemical Fabrication and Capacitance of Composite Films of Carbon Nanotubes and Polyaniline. *J. Mater. Chem.* **2005**, *15*, 2297–2303.
25. Rudge, A.; Davey, J.; Raistrick, I.; Gottesfeld, S.; Ferraris, J. P. Conducting Polymers as Active Materials in Electrochemical Capacitors. *J. Power Sources* **1994**, *47*, 89–107.
26. Wu, M. Q.; Snook, G. A.; Chen, G. Z.; Fray, D. J. Redox Deposition of Manganese Oxide on Graphite for Supercapacitors. *Electrochem. Commun.* **2004**, *6*, 499–504.
27. Barbero, C.; Tucceri, R. I.; Posadas, D.; Silber, J. J.; Sereno, L. Impedance Characteristics of Poly-*o*-aminophenol Electrodes. *Electrochim. Acta* **1995**, *40*, 1037–1040.